Available online at www.sciencedirect.com

SciVerse ScienceDirect

Ceramics International 38 (2012) 3209–3216

CERAMICS INTERNATIONAL

www.elsevier.com/locate/ceramint

Titania/hydroxyapatite bi-layer coating on Ti metal by electrophoretic deposition: Characterization and corrosion studies

Purna C. Rath, Laxmidhar Besra, Bimal P. Singh, Sarama Bhattacharjee *

Colloids & Materials Chemistry Department, Institute of Minerals and Materials Technology, (Council of Scientific & Industrial Research), Bhubaneswar – 751013, India

Received 22 November 2011; received in revised form 12 December 2011; accepted 13 December 2011
Available online 19 December 2011

Abstract

Titania–hydroxyapatite (HAp) bi-layer coating on Ti metal substrate with improved adhesion strength is fabricated by a simple two step processes: electrodeposition of Ti sol and electrophoretic deposition of HAp powder, followed by heat treatment at 800 °C. At optimized process parameters, the bi-layer developed consists of dense, thin and crystalline titania interlayer with porous, thick and crystalline HAp top layer. The heat treatment of bi-layer coating allows elemental intermixing at the interface of TiO_2 and HAp, as determined by energy dispersive X-ray spectroscopy (EDX) and Raman spectra analysis. Compared to monolithic HAp coating, the TiO_2/HAp bi-layer coating shows significant enhancement in the adhesion strength (48 MPa) as well as corrosion resistance without compromising its biocompatibility. The steep increase in adhesion strength is believed to be due to mechanical interlocking and diffusion bonding at the interface. Presence of dense titania interlayer in the bi-layer coating reduces the corrosion current in Ringer's solution to a negligible value (~100 nA).

Keywords: C. Corrosion; C. Mechanical properties; D. Apatite; E. Biomedical applications; Electrophoretic deposition

1. Introduction

Ti and Ti based alloys have been extensively used in orthopedic and dental application [1] because of their non-toxicity, biocompatibility, corrosion resistance, and good mechanical properties such as high strength, durability, light weight. Additionally, these metals exhibit less inflammation, hypersensitivity and allergic reaction when they come in contact with surrounding body tissue and fluid [2]. However, to minimize direct metal-body fluid contact and for limiting undesired metallic ions release into the body, coating of the metallic substrate with biocompatible materials such as hydroxyapatite (HAp) [$Ca_{10}(PO_4)_6(OH)_2$] is suggested [3,4] by researchers. Many in vivo studies have reported enhanced Ti implant fixation properties when coated with HAp [5–7]. Usually HAp coating on metal implant has poor adhesion. Several surface modification techniques such as sand blasting [8,9], grit blasting [10] are proposed to introduce surface roughness while chemical methods like acid treatment [11,12], alkali treatment [13], hydrogen peroxide treatment [14], etc. are used for modification of surface chemical properties for better interactions of coating material. These processes, however, improve adhesive strength only marginally. Usually high temperature driven processes such as thermal spray, plasma spray, electron beam deposition, sputter coating, pulse laser deposition tend to produce better adhesion due to melting/near melting of the coating material during deposition process that solidifies during cooling of the substrate. As an example, magnetron sputtered multilayered hydroxyapatite/titanium coating have been reported to exhibit bond strength of as high as 60 MPa [15]. But these methods could cause implant heating, leading to variation in surface coverage, coating composition, crystallinity, homogeneity and surface morphology [16].

Insertion of ceramic interlayer [17–24] on Ti and Ti based alloys prior to coating with HAp is reported to enhance coating adhesion by reducing thermal mismatch between metal and the HAp coating. Amongst various ceramic, titania has been used extensively as inter layer [20–24] before coating the metal with HAp using different techniques. In this paper, we use

* Corresponding author. Tel.: +91 674 2379326; fax: +91 674 2581637.
E-mail address: saberip@yahoo.com (S. Bhattacharjee).

0272-8842/$36.00
doi:10.1016/j.ceramint.2011.12.026

electrophoretic deposition (EPD) technique to develop the TiO_2/HAp bi-layer coating on Ti metal. EPD was used by Albayrak et al. [23] to develop TiO_2/HAp coating on Ti metal. They emphasized mainly on arresting hydroxyapatite decomposition and improving the adhesion strength by incorporating the titania interlayer. Titania interlayer thus developed using nano-size titania powder did not show any visible cracks before heat treatment, was porous after heat treatment. Moreover, the maximum adhesion strength achieved was about 20 MPa. No data was reported on any corrosion studies.

In the present study, we report preparation of TiO_2/HAp bi-layer coating on Ti metal by electrodeposition of TiO_2 sol followed by EPD of HAp powder suspension for obtaining well adhered dense and crystalline titania interlayer and porous and crystalline HAp top layer in a single heat treatment step. The heat treatment temperature was chosen in such a way that it does not decompose HAp, but at the same time densifies the inner titania layer, which is in contact with Ti surface. The novel bi-layer thus produced was found to be highly corrosion resistant, exhibiting a very low corrosion current of about 100 nA in simulated body fluids. Adhesion strength of the coating was found to be more than double of the values reported for TiO_2/HAp bi-layer coating of Albayrak et al. developed by EPD of powders [23].

2. Experimental

2.1. Materials

Ti metal sheet (purity 99%) of 0.25 mm thickness was purchased from Sigma–Aldrich, USA. They were cut into 3 mm × 1 mm pieces and used as deposition substrate during EPD. Titanium ethoxide (Sigma–Aldrich, USA), glacial acetic acid, (Qualigens, USA), anhydrous ethanol (S.d. Fine chemical Ltd., India), and hydroxyapatite powder (Berkeley Advanced Biomaterials, USA) and other reagent used for chemical synthesis were utilized without further purification.

2.2. Preparation of HAp/titania coating by electrophoretic deposition

Bi-layer TiO_2/HAp coating on Ti metal was developed by 2-stage processes. In the first step, TiO_2 coating on Ti metal was developed in two ways, by dipping in Ti sol and by electrodeposition of Ti sol where Ti metal sheet was used as the cathode, Ti sol as electrolyte and palladium as counter electrode (anode). Titania sol was prepared [25] following the established route using Ti-ethoxide as the precursor in ethanol medium. Prior to sol coating, the metal substrate was polished with silicon carbide paper (Grade P 400) and cleaned with acetone by ultra sonication, rinsed with deionized water and dried in air at room temperature. Dipping experiments were conducted where duration of dipping of Ti substrate into Ti sol was varied from 5 to 30 s, with withdrawal rate from 5 to 60 cm/min. However, coating was uneven and thin (∼1 μm), thickness of coating was independent of duration and withdrawal rate. Castro et al. [26] also observed that this method has an important limitation related with the maximum coating thickness attainable. We also observed that the coating had poor adherence after heat treatment. Hence, dipping experiments were abandoned.

In electrodeposition experiment, titania sol layer was coated onto the Ti substrate (used as cathode) by using a DC power source (Keithley source meter, model No. 2410), at a constant voltage mode of 50 V for a pre-determined deposition time. In all electrodeposition experiments, the inter-electrode distance and deposition area was maintained at 10 mm, and 100 mm^2, respectively. Experiments were carried out at different sol concentration (0.15, 0.1 and 0.05 M). The dried sol coated Ti substrates was used as cathode and Pd as counter electrode for EPD of HAp from a homogenous suspension of HAp powder in ethanol. The suspension was ultra sonicated for 30 min just before deposition at constant voltage of 100 V and varying deposition times between 10 and 60 s. Concentration of HAp in the suspension was varied from 1 to 5 wt.%. The green deposits obtained were dried slowly under gradually reducing humidity

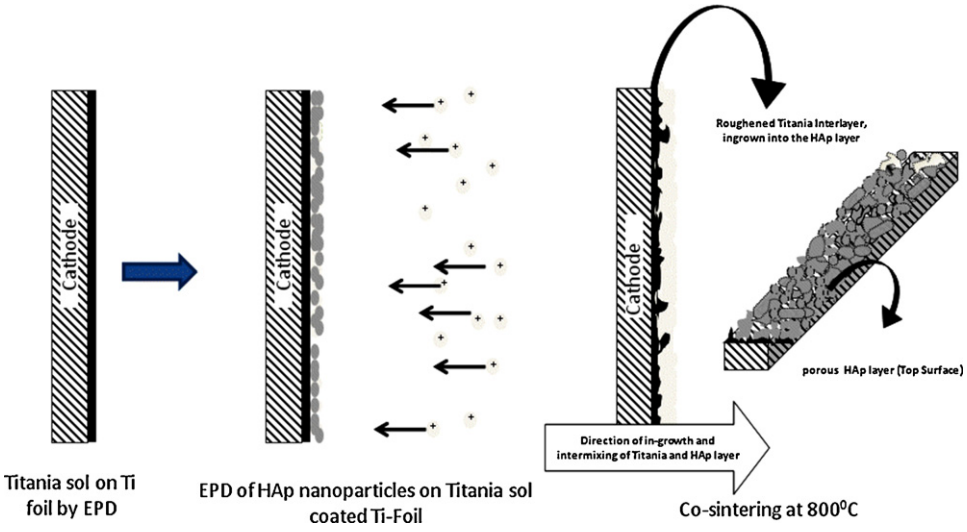

Fig. 1. Schematic representation of fabrication of adhered TiO_2/HAp bi-layer coating.

for 12 h followed by heat treatment at predetermined temperature (600–1000 °C) and time. Fig. 1 schematically presents the deposition schedule to prepare TiO_2/HAp bi-layer coating.

2.3. Physicochemical characterization

The micro-structural and morphological characterization of the sintered TiO_2/HAp bi-layer samples were carried out using Scanning Electron Microscope (SEM Model No-S-3400N, Hitachi, Japan), and phase analysis was done by X-ray Diffraction analysis (XRD Philips PAN analytical Xpert pro, Model No. PW3040/60) with a scan speed of 0.05°/s within the 2θ range of 20° and 60°. The compositional analysis of the sample was carried out by energy dispersive X-ray spectroscopy (EDS). Surface roughness and topography were characterized by Scanning Probe Microscope (SPM NANOTEC, Spain). The Raman scattering experiments were performed using a Renishaw Raman Imaging Microscope WiRE spectroscopy (Model-Invia Reflex-H33197) equipped with air cooled CCD detector. The probing spot is 2.5 μm in diameter under 1000× magnification in an optical transmission light microscope (LEICA). The 514 nm line of an Ar^+ laser was used for excitation. A 1800 grooves/nm grating was used which resulted in a spectral resolution more than 1 cm^{-1}. The spectra of TiO_2/HAp bi-layer on Ti, TiO_2 coated on Ti and heat treated HAp powders (800 °C/2 h) were measured for the range of 100–3200 cm^{-1}. The spectral region between 200 and 1200 cm^{-1} was selected for further analysis.

2.4. Adhesion test

HAp coated specimens were subjected to an adhesive strength test according to ASTM F1044-5. This test relies on a bonding agent to remove the coating from the substrate with applied shear load. The samples were glued to uncoated stainless steel with epoxy resin with a curing agent and cured at 165 °C for 1.5 h in an oven. The adhesive strength test was carried out with a universal testing machine (INSTRON 8801, USA) using a 10 kN load cell at a cross head speed of 1 mm/min. The value of the bonding strength was calculated from the fracture force over the stressed area. The adhesive strength values reported in this paper are the average of six sample tests in each group.

2.5. Corrosion studies

The electrochemical and corrosion studies on coated and uncoated samples were performed using a potentiostat (Versastat-3, Prinston Applied Research). A conventional three electrode set up was used for electrochemical measurement, with Pt as counter electrode and standard Ag/AgCl as reference electrode. The Ringer's stimulated body fluid (SBF – the aqueous solution containing 8.60 g l^{-1} NaCl, 0.33 g l^{-1} $CaCl_2$, and 0.3 g l^{-1} KCl) was used as corrosion medium. The pH of the solution was maintained at 7.4. The corrosion behavior of all the samples was carried at 37 ± 0.1 °C. The exposed area of working electrode was maintained at 1 cm^2. Open circuit potential (OCP) was monitored continuously for 2 h till the steady state was reached. The potential was increased at a rate of 1 mV/s, within a scan range of +1 V to −1 V. From the polarization curve, the corrosion potential (E_{corr}) and corrosion current density (I_{corr}) were determined by Tafel extrapolation method.

2.6. Biocompatibility test

2.6.1. Cell culture

The human osteosarcoma cell line (Saos-2) obtained from National Centre for Cell Science, Pune, India was cultured in DMEM/F12, supplemented with 10% Fetal Bovine Serum (FBS), 0.2% sodium bicarbonate and 10 ml/l antibiotic and antimycotic solution at 37 °C under a humidified atmosphere of 5% CO_2/95% air. The samples were pre-sterilized in an autoclave (121 °C, 15 lb pressure) for 15 min prior to sterilization by 70% ethanol for 30 min. Subsequently, the sample surfaces were rinsed twice with warm 1 M phosphate buffer saline (PBS) and allowed to dry in air for 1 h in a 12-well plate, maintaining sterile condition. Then the cells were seeded (20,000 cells in 100 μl of complete culture medium). They were also seeded on a glass cover slip as a control in complete culture medium in the same 12 well plate and on a Ti foil (without HAp coating). The culture plates were incubated for 2 h at 37 °C with 5% CO_2 in order to allow cells to adhere to the TiO_2/HAp bi-layer sample surface before adding 1 ml of complete culture medium to each well. The final incubation was for 48 h.

2.6.2. Mitochondrial activity

MTT [(3-(4,5-dimethylthiazol-2-yl)-2,5-diphenyltetrazolium bromide] assay was performed according to the method of Mosemann [27] in order to assess the attachment and growth of osteoblast like cell lines on TiO_2/HAp bi-layer. The cells were exposed to TiO_2/HAp bi-layer for 48 h and MTT dye (5 mg/ml) was added to each well before the completion of exposure time for 4 h. The reaction mixture resulted in the formation of formazan crystal that was dissolved in 1 ml DMSO followed by incubation for 10 min at room temperature. The solubilized formazan crystal was then transferred to a 96 well cultured plates and quantified by absorbance measurement at 550 nm in a SYNERGY-HT multi well plate reader, BIOTEK (USA) using KC4 software. The cell viability in terms of metabolically active cells was calculated using following formula:

$$\%\text{viability} = \frac{\text{mean absorbance of sample}}{\text{mean absorbance of control}} \times 100 \quad (1)$$

3. Results and discussion

3.1. Microstructural characterization

Optimization of suitable templates (titania roughened surface) for the adherence of HAp nano particles with Ti

metal was carried out by changing heat treatment schedule and varying the deposition process parameters and concentration of the titania sol during electrodeposition. Fig. 2 shows the best surface topography, having angular platelet like structure which was obtained for titania sol (0.05 M) deposited at 50 V for 5 s, followed by heat treatment at 800 °C. The titania layer thus obtained was dense and was about 4 μm thick.

Fig. 2b shows the surface topography of titania obtained at optimized condition. The precipitated titania (anatase phase) underwent phase transition to rutile above 500 °C followed by grain growth during annealing. The average surface roughness height obtained from roughness analysis was 442 nm. Fig. 3 shows the porous microstructure of top HAp surface (thickness 35 μm) obtained at optimized EPD process parameters (HAp conc. 1 wt.% in ethanol, at 100 V for 10 s deposition time.)

Fig. 4 shows the XRD patterns of heat treated (800 °C) TiO_2/HAp bi-layer and TiO_2 coating on Ti. Plot 1 shows distinguishable diffraction peaks corresponding to (0 0 2), (2 1 1), (1 1 2), (3 0 0), (2 0 2), (2 1 3) planes of crystalline HAp, along with TiO_2 and Ti peaks. Titania crystallizes in rutile phase, confirmed by the presence of (1 1 0), (1 0 1), (1 1 1), (2 1 1) diffraction peaks. No phase transition of HAp to β-TCP was observed at this heat treatment schedule.

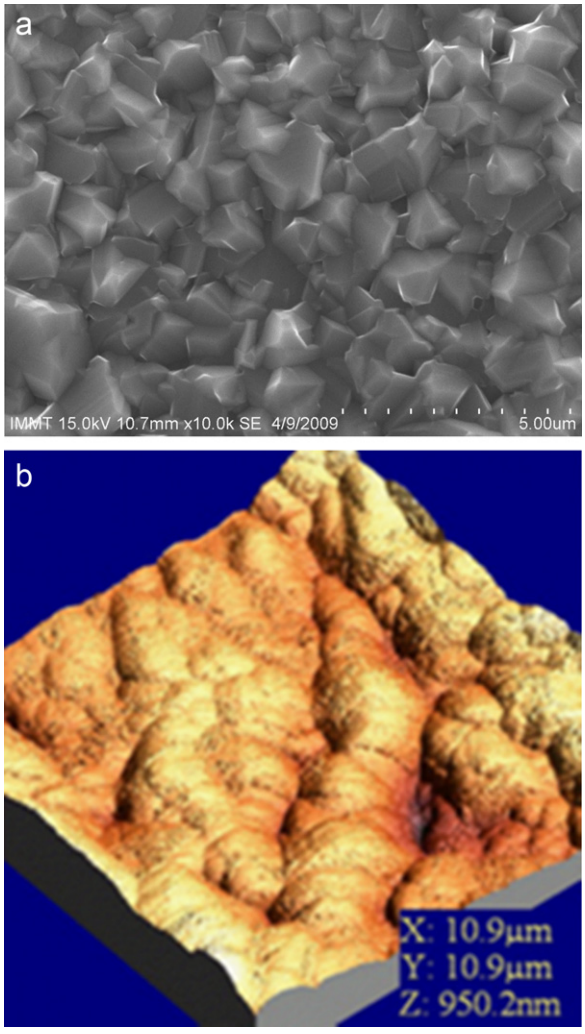

Fig. 2. (a) SEM micrograph of titania coating, EPD 50 V, 5 s, heat treatment at 800 °C. (b) AFM image [3D view] of surface topography of titania after heat treatment.

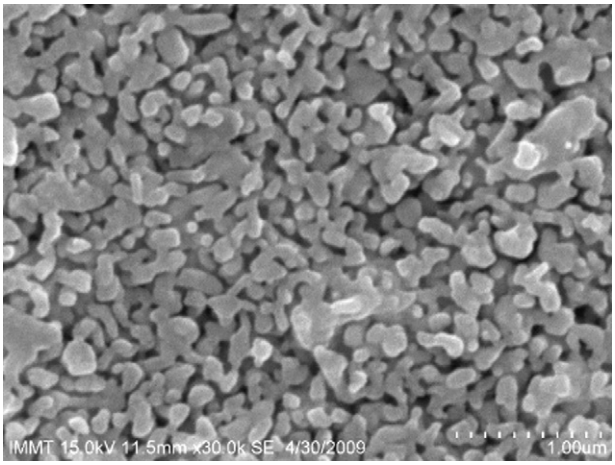

Fig. 3. SEM micrograph of HAp surface showing the porous nature.

EDX line scan analysis (Fig. 5) reveals fair intermixing of Ti, Ca, P and O at the interface of titania and HAp. This can be attributed to the deposition process and the subsequent heat treatment that allows the titania precursor and HAp nano particles intimate molecular level interactions at the interface.

3.2. Raman analysis

Raman spectrum (Fig. 6) of the heat treated (800 °C) HAp powder exhibits strong bands at 430, 590, 962, 1047, 1074 cm^{-1}.The strongest band at 962 cm^{-1} corresponds to the symmetric stretching mode ν_1 P–O of the tetrahedron PO_4^{3-}.

The other bands observed in the frequency region of 400–490 cm^{-1}, 570–625 cm^{-1}, 1020–1075 cm^{-1} are assigned to the ν_2, ν_4 and ν_3 type of internal PO_4^{3-} mode [28]. Raman spectrum of HAp/titania bi-layer (Fig. 6) shows all these bands along with TiO_2 bands (442 and 606 cm^{-1}). Additionally a band is observed at 785 cm^{-1}, which is identified as the asymmetric

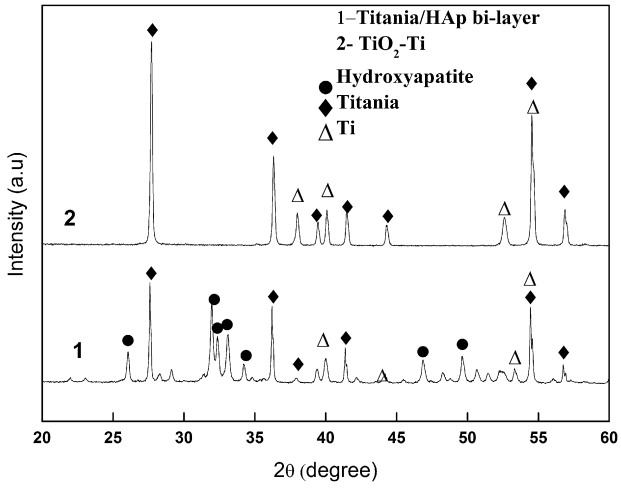

Fig. 4. XRD of HAp titania bi-layer on Ti, titania on Ti.

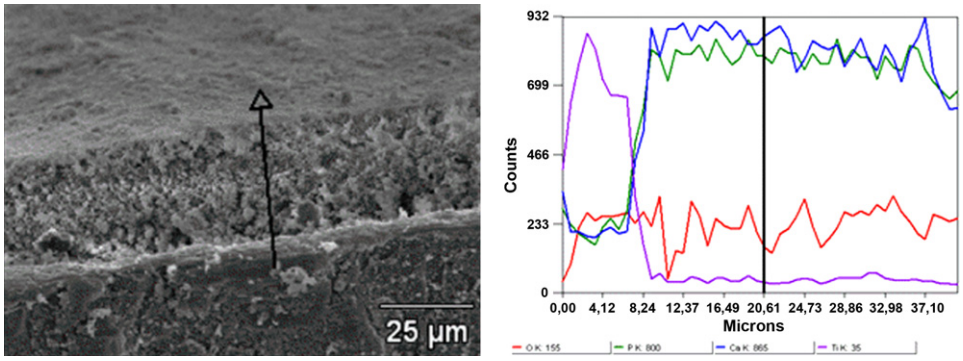

Fig. 5. EDX analysis showing good intermixing of the elements at the interface.

stretching mode of PO_4^{3-} [29]. This may be due to the interference of hydroxide group of HAp with titania at the interface.

3.3. Adhesion test

Adhesion strength of the HAp coatings on Ti without titania layer and with titania layer was 15 (±2.35) MPa and 48 (±3.67) MPa, respectively. It indicates a significant increase in adhesive properties of the coating with the introduction of titania interlayer similar to that reported by Kim et al. [21]. In this case such high bond strength is achieved due to the insertion of titania interlayer which undergone heat treatment at 800 °C. At this temperature, development of modified roughen surface topography at titania/HAp interface behaves as an anchor for the HAp nano particles. Surface roughness is recognized as an important factor in strengthening adhesion of surface coating as roughen surface provides better compatible scaffolding for adhesion via mechanical interlocking in comparison to available conventional smooth surface. Further, elemental intermixing at the interface and formation of weak bonding at the interface was facilitated by heat treatment of HAp coated on Titania sol. On the other hand, the improvement of the coating/substrate interfacial strength is due to incorporation of Titania inter-layer which has a higher chemical affinity to Ti. Hence, increase in adhesion strength from 15 to 48 MPa can be attributed to the following: (1) stronger mechanical interlocking developed due to roughened surface topography during heat treatment at the tiania and HAp interface, (2) improved wetting of top HAp coating and titania precursor before heat treatment, and (3) fair intermixing of elements at the HAp titania interface with formation of weak bond (presence of asymmetric stretching mode of PO_4^{3-} at 785 cm^{-1}) during heat treatment.

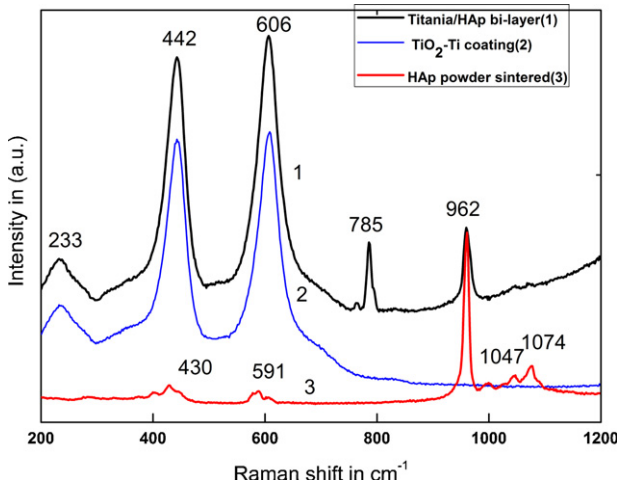

Fig. 6. Raman spectra analysis of HAp–TiO_2 bi-layer on Ti, TiO_2 coated on Ti and HAp powder (heat treated at 800 °C/2 h).

3.4. Corrosion behavior

Fig. 7a and b shows variation in open circuit potential (OCP) and cyclic potentiodynamic polarization curves (in Ringer's solution) with time for Ti metal, HAp coated and TiO_2/HAp coated Ti-metal. The corrosion parameters extracted from these curves are shown in Table 1. OCP of both the coated samples shifted significantly in the noble direction (Table 1), showing higher thermodynamic stability. For Ti metal, the passive air-formed oxide film becomes more protective after immersing in the Ringer's solution for 2 h due to the increased film thickness. Thus, the OCP increases until the film reaches its limiting protective capacity. However, for coated samples, the respective OCP stabilized much faster (Fig. 7a). Compared to the HAp coated Ti metal, the nobler OCP exhibited by TiO_2/HAp coating is due to presence of dense TiO_2 interlayer in the later sample.

Fig. 7b shows the potentiodynamic polarization curve of various coated specimens in Ringer's solution. It can be seen that below 1 V, both the coated samples have lower anodic current density compared to the bare Ti-foil as expected, while the TiO_2/HAp coating has the lowest anodic current density, showing that it has better corrosion resistance compared to HAp coated sample. The I_{corr} of bi-layer TiO_2/HAp coating (Table 1) is 104 nA (lowest value of I_{corr} reported so far for coated Ti sample), whereas HAp coated and bare Ti exhibited I_{corr} values of 1.42 and 34.657 μA/cm^2, respectively. The corrosion resistance increases by many folds in comparison to both bare substrate and HAp coated samples. Presence of dense titania interlayer along with HAp coating acts as a barrier to electrons and ions transport between the substrate and the SBF electrolyte. In addition, E_{corr} value of the specimen decreases

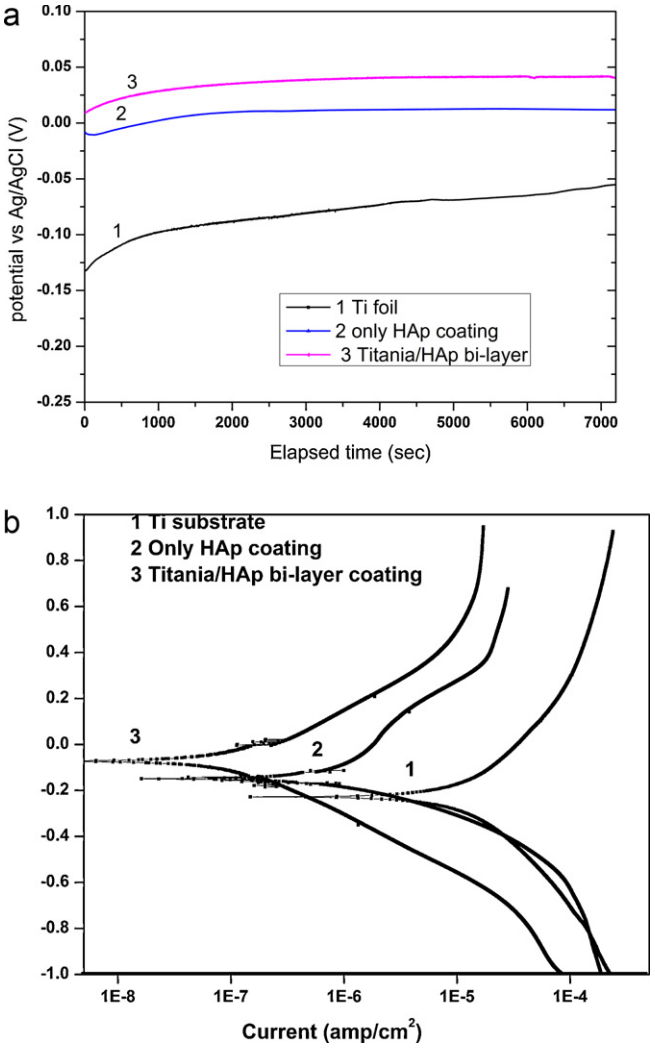

Fig. 7. (a) Variation of open circuit potential (OCP) with time of various specimen in Ringer's solution at 37 °C. (b) Potentiodynamic polarization curves for (1) Ti foil, (2) HAp coating and (3) TiO_2/HAp bi-layer coating.

from bare Ti foil (−246.7 mV) substrate to TiO_2/HAp (−75.7 mV). In other words, the corrosion potential of the bi-layer TiO_2/HAp coating is nobler and corrosion takes place at a thinner rate having lowest E_{corr} and I_{corr} values in comparison to other specimen due to the presence of dense interlayer.

Fig. 8a and b shows the SEM picture of HAp coated and TiO_2/HAp coated sample after corrosion test. HAp coated sample (Fig. 8a) shows presence of bigger pores after corrosion test compared to the bi-layer TiO_2/HAp coating (Fig. 8b). HAp-only coating developed by EPD is porous in nature. Therefore, a direct path is established between the corrosive medium and the

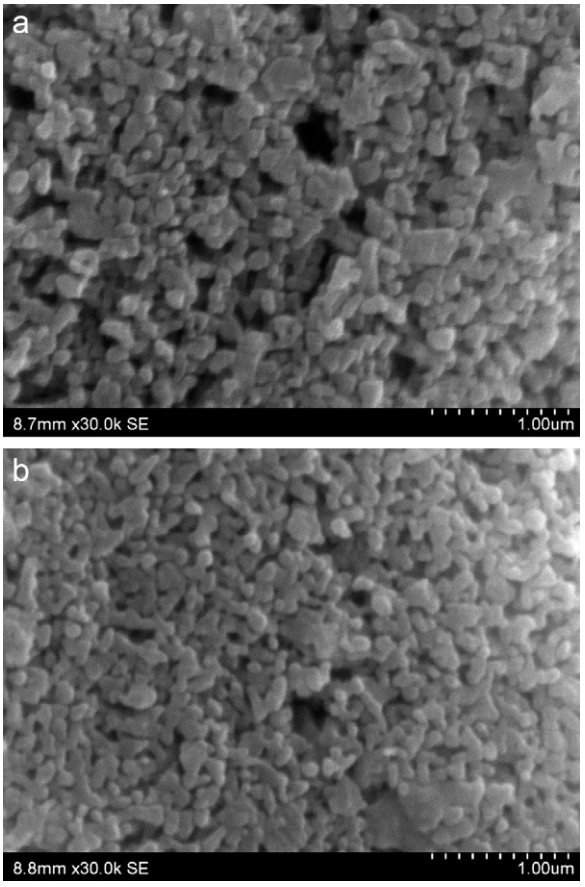

Fig. 8. (a) HAp coating on Ti and (b) TiO_2/HAp bi-layer coating on Ti after corrosion test.

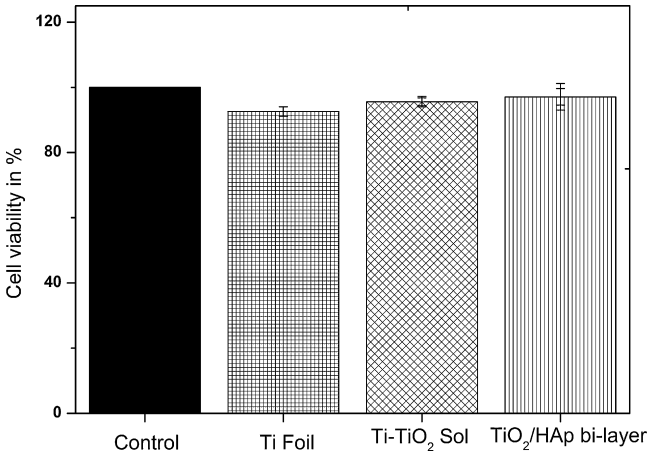

Fig. 9. Cell viability expressed by MTT assay after 48 h incubation. Data are expressed as mean ± SE from three independent experiments.

Table 1
Corrosion behavior and adhesion data of coated Ti samples.

Sample	OCP (mV)	E_{corr} (mV)	I_{corr} (μA/cm^2)	Adhesion strength (MPa)
Ti foil	−55.37	−246.69	34.66	–
HAp on Ti	11.44	−152.43	1.42	15.6
HAp–TiO_2 on Ti	38.68	−75.69	0.10	48.2

Ti metal for the HAp-only coated sample. When corrosion starts, H^+ ions are produced at the metal surface:

$$Ti + 2H_2O \rightarrow TiO_2 + 4H^+ + 4e^-$$

Owing to the poor circulation of H^+, local pH at the corrosion area becomes very acidic, and at such high H^+ concentration, HAp dissolves, forming bigger pores on the surface:

$$Ca_{10}(PO_4)_6(OH)_2 + 2H^+ \rightarrow 10Ca^{2+} + 6PO_4{}^{3-} + H_2O$$

In case of bi-layer TiO_2/HAp coating, presence of dense titania interlayer prevents direct contact of corrosive medium with the metal.

3.5. Biocompatibility test

Cell viability expressed by MTT assay after 48 h incubation is shown in Fig. 9. Data are expressed as mean ± standard error from three independent measurements. Cytotoxicity data of TiO_2/HAp bi-layer and HAp coated Ti, TiO_2 coated Ti measured after 48 h did not show any significant differences compared to the control sample (i.e. cover slip) and Ti foil. The results thus testify the high biocompatibility of the implants.

4. Conclusion

A simple, fast and cost effective Electrophoretic deposition technique is developed to obtain adhered TiO_2/HAp bi-layer coating. The TiO_2/HAp bi-layer coating exhibits enhanced adhesion strength, good corrosion resistance, and cellular biocompatibility compared to HAp-only coating. The significant increase in the adhesion strength of HAp coating is due to the mechanical interlocking of the roughened surface topography of the titania interlayer combined with diffusion bonding at the TiO_2/HAp interface. The top HAp surface is crystalline and porous, while the intermediate titania layer is crystalline and dense. Existence of such a dense interlayer along with crystalline nature of HAp particles marks a drastic improvement in decreasing corrosion of the TiO_2/HAp bi-layer coating which exhibits very low corrosion current in the nano-ampere range. The coated Ti samples are highly bioactive in nature. The advantage of this two steps EPD process is that both the deposition steps are cathodic, that reduces electrode erosion and improves adhesion of coating by directed electric field compared to anodic deposition [30]. During deposition of HAp, no charge modifying agent is added to the suspension which helps in maintaining the purity of coating.

Acknowledgements

The authors gratefully acknowledge the financial support from the Network project: Nanomaterials & Nanodevices for the Applications in Health & Diseases, CSIR, New Delhi. Special thanks to Dr. Alok Dhawan, scientist, IITR, Lucknow, India, for carrying out the bio-compatibility tests and Prof B. K. Mishra, Director, IMMT, Bhubaneswar, for permission to publish this paper.

References

[1] L. Xuanyong, P.K. Chu, C. Ding, Surface modification of titanium, titanium alloys, and related materials for biomedical applications, Mater. Sci. Eng. Rep. 47 (2004) 49–121.
[2] C. Ohthuki, A. Osaka, H. Lida, K. Ohta, Biocompatible titanium implant. US Patent 58,85,612 (1999).
[3] A. Duran, A. Conde, C.A. Gomez, T. Dorado, C. Garcıa, S. Cere, Sol–gel coatings for protection and bioactivation of metals used in orthopaedic device, J. Mater. Chem. 14 (2004) 2282–2290.
[4] M.H. Fathi, F. Azam, Novel hydroxyapatite/tantalum surface coating for metallic dental implant, Mater. Lett. 61 (2007) 1238–1241.
[5] L.L. Hench, Bioceramics: from concept to clinic, J. Am. Ceram. Soc. 74 (1991) 1485–1510.
[6] R.Z. Legeros, Biodegradation and bioresorption of calcium phosphate ceramics, Clin. Mater. 14 (1993) 65–88.
[7] C.F. Koch, S. Johnson, D. Kumar, M. Jelinek, D.B. Chrisey, A. Doraiswamy, C. Jin, R.J. Narayan, I.N. Mihailescu, Pulsed laser deposition of thin films, Mater. Sci. Eng. C 27 (2007) 484–494.
[8] M. Multigner, E. Frutos, J.L. Gonzalez, J.A. Jimenez, P. Marín, J. Ibanez, Influence of the sandblasting on the subsurface microstructure of 316LVM stainless steel: implications on the magnetic and mechanical properties, Mater. Sci. Eng. C 29 (2009) 1357–1360.
[9] D. Li, B. Liu, Y. Han, K. Xu, Effects of a modified sand blasting surface treatment on topographic and chemical properties of titanium surface, Implant Dent. 10 (2001) 59–64.
[10] Y.W. Kim, Surface modification of Ti dental implants by grit-blasting and micro-arc oxidation, Mater. Manuf. Processes 25 (2010) 307–310.
[11] A. Nanci, J.D. Wuest, L. Peru, P. Brunet, V. Sharma, S. Zalzal, M.D. McKee, Chemical modification of titanium surfaces for covalent attachment of biological molecules, J. Biomed. Mater. Res. 40 (1998) 324–335.
[12] C. Viornery, Y. Chevolot, D. Leonard, B.O. Aronsson, P. Pechy, H.J. Mathieu, P. Descouts, M. Gratzel, Surface modification of Titanium with phosphonic acid to improve bone bonding: characterization by XPS and ToF-SIMS, Langmuir 18 (2002) 2582–2589.
[13] W.F. Ho, C.H. Lai, H.C. Hsu, S.C. Wu, Surface modification of a Ti–7.5Mo alloy using NaOH treatment and Bio-glass coating, J. Mater. Sci. Mater. Med. 21 (2010) 1479–1488.
[14] B. Walivaara, I. Lundstrom, P. Tengvall, An in vitro study of H_2O_2-treated titanium surfaces in contact with blood plasma and a stimulated body fluid, Clin. Mater. 12 (1993) 141–148.
[15] S. Ding, Properties and immersion behavior of magnetron-sputtered multi-layered hydroxyapatite/titanium composite coatings, Biomaterials 24 (2003) 4233–4238.
[16] Z. Zhang, T.D. Xiao, Coatings, coated articles and methods of manufacture thereof. US Patent 73,20,799 B2 (2008).
[17] W.Z. Jun, H.L. Ping, C.Z. Zhang, Fabrication and characterization of hydroxyapatite/Al_2O_3 biocomposite coating on Titanium, Trans. Nonferr. Met. Soc. China 16 (2006) 259–266.
[18] Y.C. Yang, B.Y. Chouc, Bonding strength investigation of plasma-sprayed HA coatings on alumina substrate with porcelain intermediate layer, Mater. Chem. Phys. 104 (2007) 312–319.
[19] H.C. Man, K.Y. Chiu, F.T. Cheng, K.H. Wong, Adhesion study of pulsed laser deposited hydroxyapatite coating on laser surface nitrided titanium, Thin Solid Films 517 (2009) 596–601.
[20] X. Nie, A. Leyland, A. Matthews, Deposition of layered bioceramic hydroxyapatite/TiO_2 coatings on titanium alloys using a hybrid technique of micro-arc oxidation and electrophoresis, Surf. Coat. Technol. 125 (2000) 407–414.
[21] H.W. Kim, Y.H. Koh, L.H. Li, S. Lee, H.E. Kim, Hydroxyapatite coating on titanium substrate with titania buffer layer processed by sol–gel method, Biomaterials 25 (2004) 2533–2538.
[22] Y.P. Lu, M.S. Li, S.T. Li, Z.G. Wang, R.F. Zhu, Plasma-sprayed hydroxyapatite + titania composite bond coat for hydroxyapatite coating on titanium substrate, Biomaterials 25 (2004) 4393–4403.
[23] O. Albayrak, O.E. Atwani, S. Altintas, Hydroxyapatite coating on titanium substrate by electrophoretic deposition method: effects of titanium dioxide

inner layer on adhesion strength and hydroxyapatite decomposition, Surf. Coat. Technol. 202 (2008) 2482–2487.

[24] P. Rajesh, C.V. Muraleedharan, M. Komath, H. Verma, Pulsed laser deposition of hydroxyapatite on titanium substrate with titania interlayer, J. Mater. Sci. Mater. Med. 22 (2011) 497–505.

[25] Y. Lin, G.S. Wu, X.Y. Yuan, T. Xie, L.D. Zhang, Fabrication and optical properties of TiO_2 nano wire arrays made by sol–gel electrophoresis deposition in to anodic alumina membranes, J. Phys.: Condens. Matter 15 (2003) 2917–2922.

[26] Y. Castro, B. Ferrari, R. Mureno, A. Duran, Coatings produced by electrophoretic deposition from nano-particulate silica sol–gel suspensions, Surf. Coat. Technol. 182 (2004) 199–203.

[27] T. Mosemann, Rapid colorimetric assay for cellular growth and survival: application to proliferation and cytotoxicity assays, J. Immunol. Methods 65 (1983) 55–63.

[28] Z. Iqbal, V.P. Tomaselli, O. Fahrenfeld, K.D. Moller, F.A. Ruszala, E.J. Kostiner, Polarization Raman scattering and low frequency infrared study of hydroxyapatite, J. Phys. Chem. Solids 38 (1977) 923–927.

[29] I. Rehrnan, R. Smith, L.L. Hench, W. Bonfield, Structural evaluation of human and sheep bone and comparison with synthetic hydroxyapatite by FT-Raman spectroscopy, J. Biomed. Mater. Res. 29 (1995) 1287–1294.

[30] L. Besra, T. Utchikosi, T.S. Suzuki, Y. Sakka, Bubble-free aqueous electrophoretic deposition (EPD) by pulse-potential application, J. Am. Ceram. Soc. 91 (2008) 3154–3159.